Journal of Solid State Chemistry **164,** 313–319 (2002)
doi:10.1006/jssc.2001.9476, available online at http://www.idealibrary.com on IDEAL®

Field-Induced Magnetic Properties in $RCrO_4$ Oxides (R = Pr, Gd, Tb, Tm, and Yb)

E. Jiménez, J. Isasi, and R. Sáez-Puche[1]

Departamento de Química Inorgánica, Facultad de Ciencias Químicas, Universidad Complutense de Madrid, 28040 Madrid, Spain

Received August 7, 2001; in revised form November 5, 2001; accepted December 3, 2001; published online February 12, 2002

$RCrO_4$ oxides (R = Pr, Gd, Tb, Tm, and Yb) have been synthesized at 773 K using the corresponding nitrates as precursors. X-ray diffraction data reveal that these samples are single phases and crystallize with the zircon-type structure, showing tetragonal symmetry, space group $I4_1/amd$. All the compounds are antiferromagnetic and the Néel temperature, which depends on the R^{3+} ion, takes values lower than 30 K. The presence of a canting appears to be responsible for the negative values of the magnetic susceptibility found below the compensation temperature. This uncommon phenomenon is named reversal of magnetization. It is field-dependent, being suppressed at 500 Oe for the $TmCrO_4$ compound. The highest value of the compensation temperature (24 K) corresponds to the $YbCrO_4$ oxide. A metamagnetic transition has been observed in all cases at critical fields ranging from 225 Oe ($GdCrO_4$) to 1600 Oe ($YbCrO_4$).

Key Words: **lanthanide chromates; zircon-type structure; antiferromagnetism; reversal of magnetization; metamagnetism.**

1. INTRODUCTION

Previous studies concerning the family of oxides $RCrO_4$ (R = Nd–Lu and Y) reveal that they crystallize with the zircon-type structure, space group $I4_1/amd$ (1). This structure can be described as built up by (RO_8) bisdisphenoid polyhedra forming edge-sharing zig-zag chains along the a-axis. Such chains are connected to one another in the c-direction by common edges of the (CrO_4) tetrahedra units, as can be observed in Fig. 1. On the other hand, $LaCrO_4$ presents the monazite structure (2). $PrCrO_4$ is dimorphic and very recently we have been able to isolate both the zircon and monazite (3) polymorphs as pure phases using specific synthesis conditions.

The coexistence of two paramagnetic cations, namely Cr^{5+} and R^{3+}, in these compounds constitutes an adequate scenario to study the 3d–4f magnetic interactions and the important role that the rare earth anisotropy plays in the magnetic properties. Magnetic susceptibility and magnetization measurements applying magnetic fields higher than 1000 Oe led to the assignment of a ferromagnetic behavior to most of these oxides (4). However, our previous results indicate that such behavior is clearly induced by the external magnetic field. In fact, the $RCrO_4$ compounds (R = Sm, Eu, Er, and Lu) can be classified as antiferromagnetic materials (5). The strong influence of the crystal field on the ground term $^4I_{9/2}$ of the Nd^{3+} ion at low temperatures appears to be the responsible for the anomaly found in the susceptibility vs temperature plot of the $NdCrO_4$, rather than the antiferromagnetic ordering recently proposed with $T_N = 25.2$ K (6). The aim of this research work is to study thoroughly the magnetic properties of the $RCrO_4$ oxides (R = Pr, Gd, Tb, Tm, and Yb) employing different magnetic field strengths in a wide range of temperatures.

2. EXPERIMENTAL

In this study, we have prepared the samples by heating the stoichiometric amounts of $R(NO_3)_3 \cdot 6H_2O$ and $Cr(NO_3)_3 \cdot 9H_2O$, following the thermal scheme: 30 min at 433 K, 30 min at 473 K, and 60 min at 773 K. An oxygen flow has been used in order to stabilize the 5+ oxidation state in the chromium ion. The reaction takes place according to

$$R(NO_3)_3 \cdot 6H_2O + Cr(NO_3)_3 \cdot 9H_2O = RCrO_4 + 6NO_2 + 15H_2O.$$

The obtained samples are green-colored, and the X-ray diffraction patterns show the existence of the zircon polymorph as a single phase in all cases.

Powder X-ray diffraction patterns were registered at a rate of 0.1° (2) min^{-1} using a Philips X'Pert MPD, Ni-filtered Cu $K\alpha$ radiation. A step scan of 0.04° (2) between 10°–120° and a counting time of 15 s for each step were

[1]To whom the correspondence should be addressed. Fax: +34- 91 394 43 52. E-mail: rsp92@quim.ucm.es.

0022-4596/02 $35.00

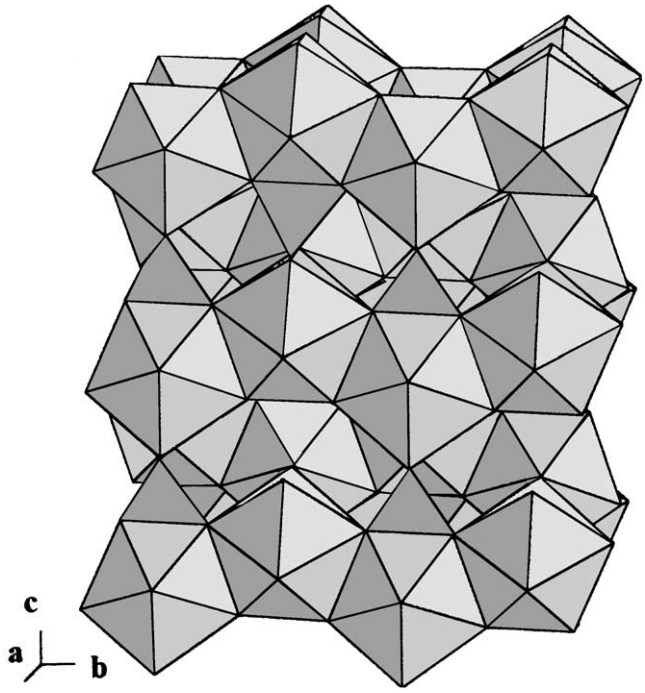

FIG. 1. Perspective view of the zircon-type structure, showing the chains of edge-sharing (RO_8) bisdisphenoid polyhedra along the *b*-axis connected by CrO_4 tetrahedra.

employed. Rietveld full-profile refinement was done with the FULLPROF program (7).

AC and DC magnetic susceptibility measurements were performed using a Quantum Design XL-SQUID magnetometer in the temperature range of 1.7–300 K at different magnetic fields. The susceptibilities were corrected for ionic diamagnetism (8). AC susceptibility measurements have been carried out at a frequency of 400 Hz with an amplitude of 1 Oe at zero magnetic fields. χ_{DC} measurements were performed after the sample was cooled to 2 K in zero field (ZFC). Decreasing the temperature in the presence of the required magnetic field allowed out field cooling measurements (FC) to be made. The magnetization was measured at different temperatures in the magnetic field range of 0–5 T.

3. RESULTS AND DISCUSSION

X-ray diffraction data reveal that all the samples are isostructural and they have been refined according to the zircon-type structure, S.G. $I4_1/amd$. As a representative example, Fig. 2 shows the pattern of the $TbCrO_4$ compound. The FULLPROF refinement results for the different $RCrO_4$ oxides are summarized in Table 1. R^{3+} ions are placed in 4a sites (0, $\frac{3}{4}$, $\frac{1}{8}$), Cr^{5+} in 4*b* sites (0, $\frac{1}{4}$, $\frac{3}{8}$), and oxygen in 16*h* sites (0, *y*, *z*). The main *d*(Cr–O) and *d*(R–O) distances are also included in Table 1. The rare earth ions are centered in their respective distorted bisdisphenoids in octacoordination, while the coordination of the chromium ion is tetrahedral. The size of the (RO_8) bisdisphenoid polyhedron diminishes progressively along with the size of the R^{3+} ion in going from Pr^{3+} to Yb^{3+}, while the size of the (CrO_4) tetrahedra evolves in the opposite direction. This fact can be explained by taking into account the competition to form the *R*–O and Cr–O bonds. The smaller size of the R^{3+} ion yields a more acidic Lewis character, presenting more affinity for the electrons in the *R*–O bonds. Consequently, the Cr–O bonds become weaker, justifying the progressive increase of the Cr–O

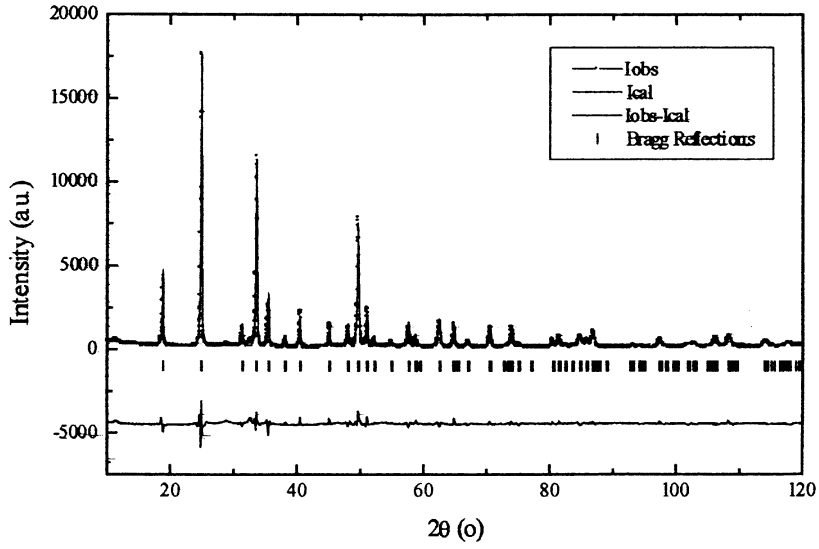

FIG. 2. X-ray diffraction pattern for the $TbCrO_4$ compound.

TABLE 1
Rietveld Refinement Data for RCrO$_4$, R = Pr, Gd, Tb, Tm, and Yb

R	a/Å	c/Å	y	z	R_{wp}	R_B	d(Cr–O)/Å	d(R–O)/Å
Pr[a]	7.341(7)	6.427(1)	0.429(1)	0.221(4)	15.4	10.6	1.643(5) × 4	2.585(4) × 4 2.436(5) × 4
Gd	7.203(3)	6.319(2)	0.424(1)	0.219(6)	13.9	6.05	1.652(5) × 4	2.513(3) × 4 2.422(5) × 4
Tb	7.159(3)	6.283(9)	0.432(7)	0.208(3)	14.1	6.05	1.676(2) × 4	2.469(6) × 4 2.330(8) × 4
Tm	7.061(1)	6.216(4)	0.404(6)	0.210(5)	17.5	7.05	1.692(7) × 4	2.395(2) × 4 2.281(1) × 4
Yb	7.037(6)	6.204(2)	0.435(1)	0.200(1)	15.8	3.74	1.700(3) × 4	2.403(1) × 4 2.258(1) × 4

[a]See Ref. (2). *Note*. $R_{wp} = [100 \sum_i (Y_i - Y_{ci})^2 / \sum_i (Y_i)^2]^{1/2}$. $R_B = 100 \sum_i (I_i - I_{ci}) / \sum_i (I_i)$

distance along the RCrO$_4$ series of oxides. According to the above discussion, the a and c lattice parameters of these phases decrease linearly with the reduction of the ionic radius of the rare earth from Pr to Yb, due to the lanthanide contraction.

Magnetic susceptibility data follow the Curie–Weiss law,

$$\chi = C/(T - \Theta),$$

in a wide range of temperatures 300–50 K in all cases. The obtained values of the effective magnetic moments of the R^{3+}, after discounting the Cr^{5+} magnetic contribution (1.67 μ_B), agree with the theoretical ones calculated by Hund's equation (see Table 2). However, at temperatures below 50 K, the magnetic behavior of these samples depends on the particular rare earth cation present in each RCrO$_4$ oxide. Besides that, the magnetic susceptibility becomes field-dependent.

As the temperature continues to decrease from 50 K, a sudden increase is observed in the magnetic susceptibility, followed by the presence of a net maximum (see Fig. 3). The mentioned increase can be attributed to ferromagnetic interactions in the Cr^{5+} sublattice. However, at the net maximum, characterized by the Néel temperature (T_N), the R^{3+}–O–Cr^{5+} and R^{3+}–O–Cr^{5+}–O–R^{3+} interactions become operative. This fact gives rise to a three-dimensional antiferromagnetic ordering in which both sublattices are involved.

TABLE 2
Experimental (μ_{exp}) and Theoretical (μ_t) Magnetic Moments, Weiss Constant (θ), and Néel Temperature (T_N) for the RCrO$_4$ Oxides, R = Pr, Gd, Tb, Tm, and Yb

R	μ_{exp}[a]/μ_B	μ_t/μ_B	T_N/K	θK
Pr	3.60	3.52	8.8	0.09
Gd	7.90	7.94	21.0	−2.45
Tb	9.60	9.70	22.0	−7.25
Tm	7.58	7.60	19.0	9.01
Yb	4.61	4.50	25.0	0.20

[a]After discounting the Cr^{5+} magnetic contribution.

We have also measured the AC susceptibility at different temperatures and, in all cases, a narrow peak is observed in the χ_{AC}' vs T plot, whose temperature exactly conforms with the Néel temperature previously obtained in the DC magnetic susceptibility measurements. Figure 4 shows the χ_{AC} vs T plot for the YbCrO$_4$ oxide as a representative example.

The magnetic susceptibility decreases as the temperature is lowered from the Néel temperature, taking a zero value at the so-called compensation temperature (T_{comp}). As in the case of the T_N, the T_{comp} is dependent on both the rare earth cation and the magnetic field employed in the measurements (see Fig. 3 and Table 3). Further cooling leads to negative values of the magnetic susceptibility. During past decades, several groups have reported similar anomalous diamagnetism caused by a reversal of the ferromagnetic component of a canted antiferromagnet and this unusual phenomenon is named reversal magnetization, which indicates that the direction of the magnetization is the reverse of that of the applied magnetic field below the compensation temperature (9–13). Recently, Ren *et al.* (14) have been found reversal magnetization in single crystals of YVO_3. The mechanism to explain this phenomenon is related to the competition of the single V^{3+} magnetic anisotropy and the antisymmetric Dzialoshinsky–Moriya interaction. In the case of these RCrO$_4$ oxides, this fact can be explained by the presence of a weak ferromagnetic component or canting arising from the imperfect alignment of the magnetic moments corresponding to the Cr^{5+} and R^{3+} ions in the antiferromagnetic state. As the temperature is decreased from the Néel temperature, such canting tends to align antiparallel to the external magnetic field. The driving force for this behavior is a molecular field (H_m), probably stemming from the Cr^{5+} sublattice. When the projection of the canting in the direction of

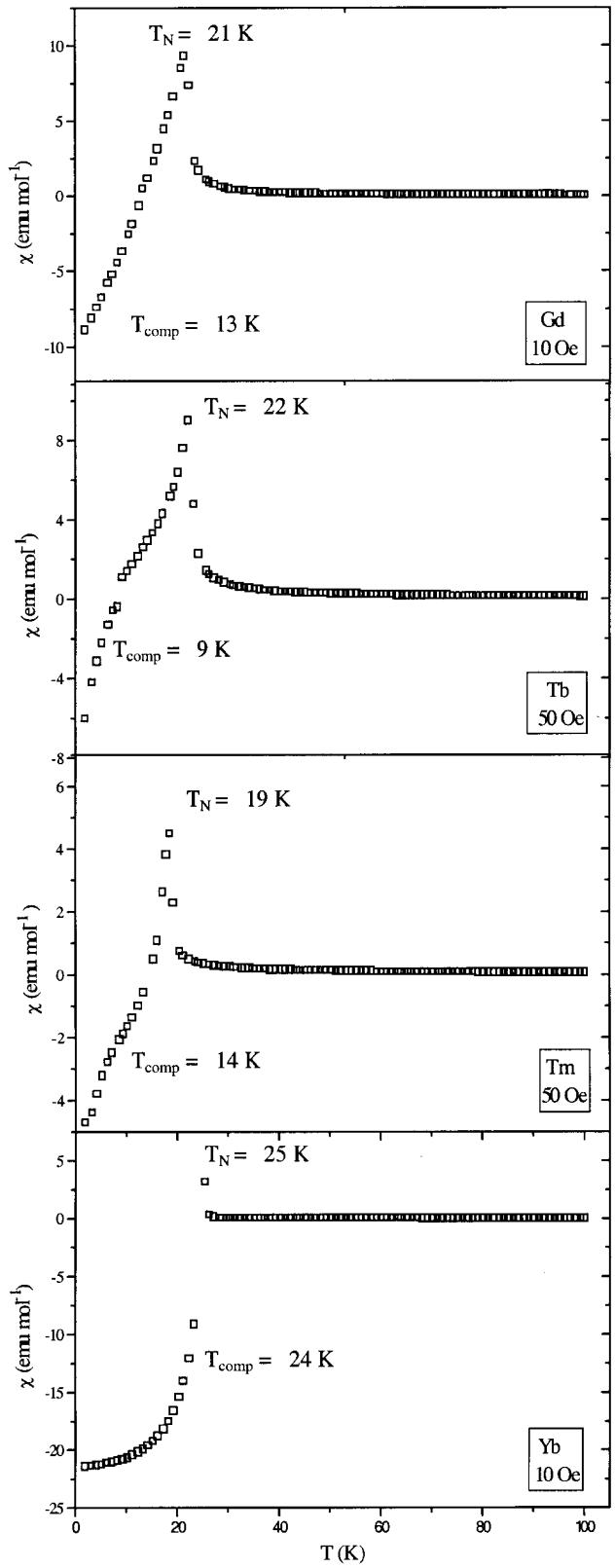

FIG. 3. DC magnetic susceptibility of the RCrO$_4$ oxides (R = Gd, Tb, Tm, and Yb).

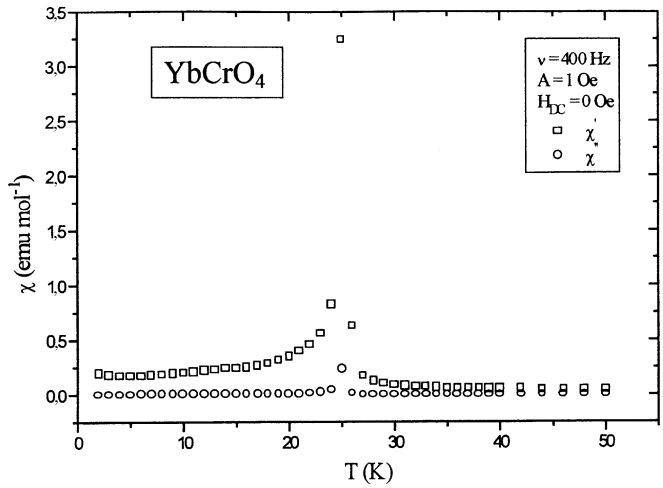

FIG. 4. AC magnetic susceptibility of the $YbCrO_4$ oxide.

the applied magnetic field compensates the latter, the T_{comp} is reached. At 2 K, that ferromagnetic component is aligned opposite to the external magnetic field, reaching saturation in the case of the $YbCrO_4$ oxide, as can be observed in Fig. 3.

Below the Néel temperature, substantial differences are observed between the measurements made upon warming after field cooling the sample in the required magnetic field (FC) and those made after zero-field cooling the sample (ZFC). When the FC process is employed, the ferromagnetic component of the Cr^{5+} sublattice above the Néel temperature is quenched, attaining the saturation state at temperatures not far from 2 K. In this case, the complex magnetic behavior described previously in the ZFC process is completely masked. The FC and ZFC magnetic data of the $TbCrO_4$ oxide at 10 Oe are shown in Fig. 5 as a representative example. The reason for the difference between the ZFC and FC measurements is that in the FC cycle the particles are magnetically annealed so that their net magnetization moments will orient in the direction of the applied magnetic field, while in the ZFC procedure the particles will be magnetically ordered below T_N with their

TABLE 3

Compensation Temperature (T_{comp}), Magnetic Moment (μ), Critical Field (H_c), and Saturation Magnetic Moment (M) for the RCrO$_4$ Oxides, R = Pr, Gd, Tb, Tm, and Yb

R	T_{comp}/K	μ (2 K, 0 Oe)/μ_B	H_c(2 K)/Oe	M (2 K, 5 T)/μ_B
Pr	8[a]	-2.4×10^{-3}	400	0.09
Gd	13[a]	-1.5×10^{-2}	225	7.0
Tb	9[b]	1.14	975	3.5
Tm	14[b]	-1.5×10^{-2}	875	2.3
Yb	24[a]	0.14	1600	0.5

[a]At 10 Oe. [b]At 50 Oe.

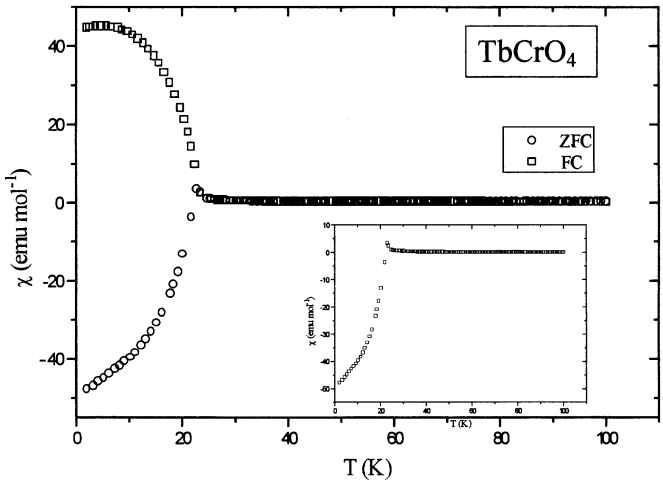

FIG. 5. FC and ZFC magnetic susceptibility of the $TbCrO_4$ oxide at 10 Oe. The inset is the ZFC magnetic susceptibility, where the net maximum can be clearly visualized.

ferromagnetic component randomly distributed. This net moment is then antiparallel aligned for low applied field values.

Figure 6 displays the ZFC process of the $TmCrO_4$ at different magnetic fields. When the applied magnetic field is high enough, it overcomes the molecular field, and the reversal of magnetization phenomenon is totally suppressed. For instance, such is the case of the $TmCrO_4$ oxide when the external magnetic field is 500 Oe. Moreover, its Néel temperature value keeps approximately constant between 10 and 100 Oe. However, above 100 Oe, the T_N starts to decrease, as a consequence of the perturbation of the antiferromagnetic state. At 1 T, the net maximum has been obliterated and the trend of the magnetic susceptibility corresponds with a ferromagnetic state. The values of T_N and T_{comp} as functions of the applied magnetic field, as well as the χ_{ZFC} and χ_{FC} at 2 K, for the $TmCrO_4$ compound are collected in Table 4.

TABLE 4
Néel Temperature (T_N), Compensation Temperature (T_{comp}), Zero-Field Cooling Susceptibility (χ_{ZFC}), and Field-Cooling Susceptibility (χ_{FC}) for the $TmCrO_4$ Oxide at Different Magnetic Fields

H (Oe)	T_N/K	T_{comp}/K	χ_{ZFC}(2 K)/emu.mol^{-1}	χ_{FC} (2 K)/emu.mol^{-1}
10	18.0	8.5	−1.9	56.1
50	18.6	14.4	−4.7	40.1
100	18.0	8.2	−1.9	29.2
500	16.3	—	2.5	13.3
1000	7.0	—	1.5	—
10,000	—	—	5.5	—

As the $TbCrO_4$ oxide presents the highest value of χ_{ZFC} at 2 K (see Fig. 5), it is expected that it possesses the largest ferromagnetic component or canting. This hypothesis is confirmed by the magnetization measurements (see Fig. 7). At a zero value of the external magnetic field, this compound presents a magnetization value of 1.14 μ_B. As the moment provided by the ordered Cr^{5+} sublattice cannot exceed 1 μ_B, the Tb^{3+} sublattice must be inevitably involved in the canting of the magnetic structure. Moreover, the ytterbium phase possesses a value of 0.14 μ_B at zero magnetic fields, while the remaining oxides display small negative values of the magnetization.

The magnetization vs applied magnetic field plots of the ytterbium and gadolinium chromates are presented in Figs. 8 and 9, respectively. In all cases, another magnetic phenomenon can be clearly appreciated in the mentioned

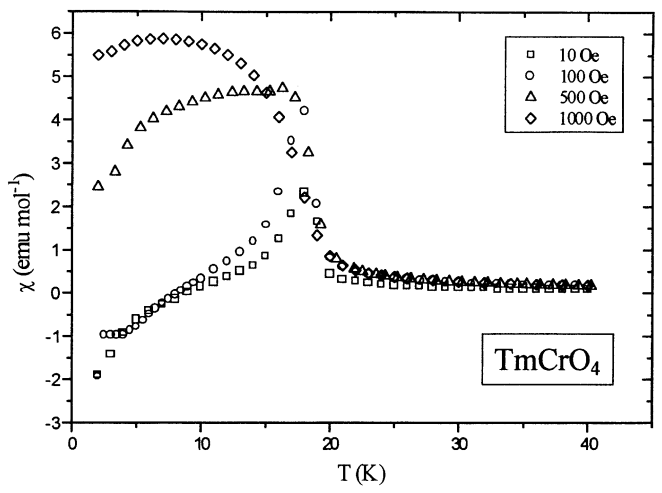

FIG. 6. ZFC magnetic susceptibility of the $TmCrO_4$ at different magnetic fields.

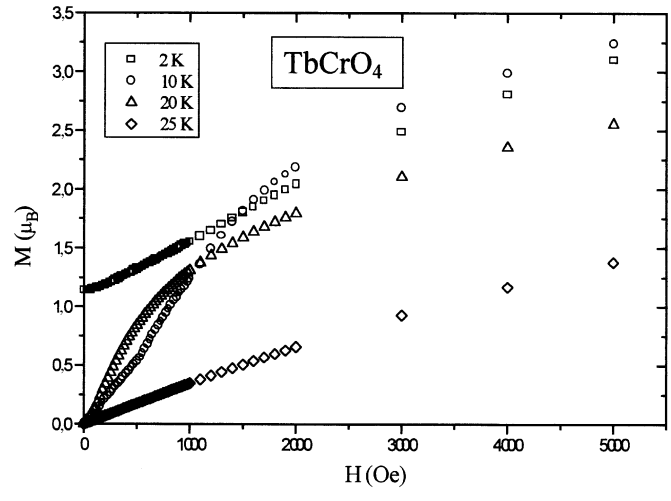

FIG. 7. Magnetization vs magnetic field plot of the $TbCrO_4$ oxide in the range of 0–5000 Oe.

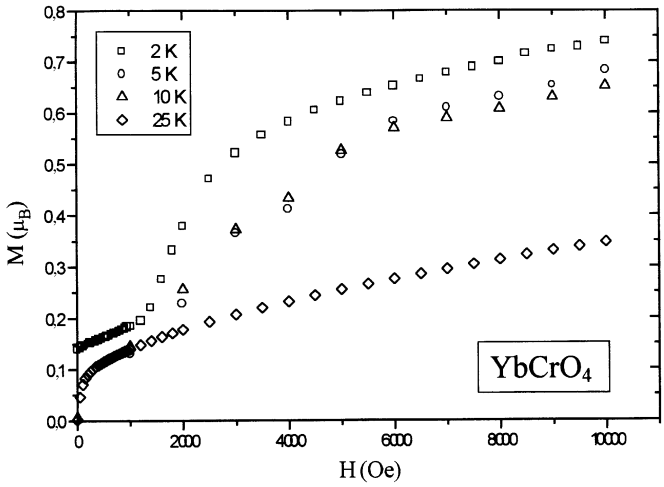

FIG. 8. Magnetization vs magnetic field plot of the $YbCrO_4$ oxide in the range of 0–1 T.

figures. At low magnetic fields, the M vs H plots follow a linear variation, which corresponds with an antiferromagnetic state. However, when the external magnetic field exceeds a critical value, termed the critical field (H_c), the R^{3+}–O–Cr^{5+} and R^{3+}–O–Cr^{5+}–O–R^{3+} interactions are perturbed and a metamagnetic transition takes place. The consequence of this behavior is a sudden jump in the magnetization. The value of that critical field depends on the measurement temperature. For the purpose of determining the critical field at different temperatures, the dM/dH vs H plot is displayed as an inset in Fig. 9 for the case of the $GdCrO_4$ oxide. As can be observed, the magnetic field that is necessary for the metamagnetic transition to occur decreases notably as the temperature becomes higher. It is worth noting that the lowest value of H_c (225 Oe) is

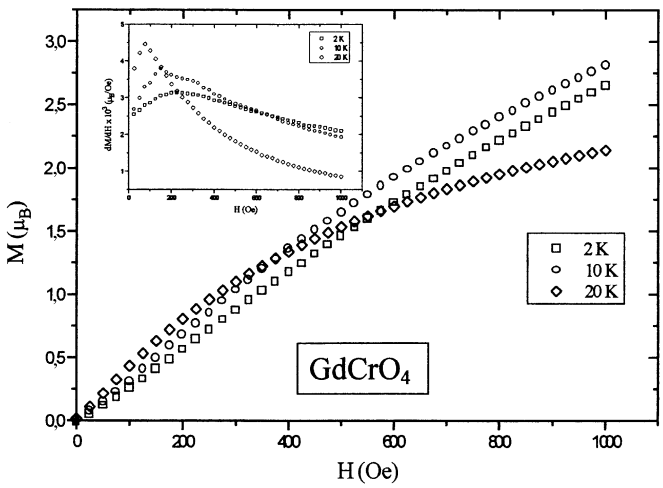

FIG. 9. Magnetization vs magnetic field plot of the $GdCrO_4$ oxide in the range of 0–1000 Oe.

attained for the $GdCrO_4$ derivate, which can be ascribed to the lack of magnetic anisotropy of the Gd^{3+} ion, which possesses $^8S_{7/2}$ as the ground term. Below the Néel temperature, substantial differences are observed between the measurements made upon warming after field cooling the sample in the required magnetic field (FC) and those made after zero-field cooling the sample (ZFC).

When the temperature is higher than the Néel temperature, the M vs H plot corresponds with a ferromagnetic material and, consequently, no metamagnetic transition is observed. Such is the case of the $TbCrO_4$ compound at 25 K (its T_N value is 22 K) (Fig. 7). This fact serves to confirm the magnetic ordering in the Cr^{5+} sublattice above the Néel temperature.

4. CONCLUSIONS

The magnetic properties of an extended number of isostructural $RCrO_4$ oxides have been systematically studied. We have found that these oxides behave as canted antiferromagnets and their estimated Néel temperatures are dependent on the R^{3+} ion. The net magnetization observed in the samples is caused by a canting of the nearly antiferromagnetic arrangements of the spins of both Cr^{5+} and R^{3+} sublattices. Below the Néel temperature, which is dependent on the rare earth, at an applied magnetic field lower than 200 Oe, the magnetization decreases monotonically with the temperature, reaching negative values after passing the so-called compensation temperature. This anomalous diamagnetism, called reversal magnetization, is caused by a reversal of the ferromagnetic component arising from the canted antiferromagnetic behavior that presents these oxides. Metamagnetic transitions have been detected in all cases at relatively weak magnetic fields ranging from 225 Oe in the case of $GdCrO_4$ to 1600 Oe for $YbCrO_4$, which clearly reflects the effect of the crystal field anisotropy associated with the ground term of the corresponding rare earth trivalent cation.

ACKNOWLEDGMENT

We thank DGICYT for financial support, under the project MAT-2000-0753-C02-01.

REFERENCES

1. G. Buisson, F. Bertaut, and J. Mareschal, *C. R. Acad. Sc. Paris* **259,** 411(1964).
2. J. D. Carter, H. U. Anderson, and M. G. Shumsky, *J. Mater. Sci.* **31,** 551 (1996).
3. E. Jiménez, J. Isasi, and R. Sáez-Puche, *J. Alloys Comp.* **323–324,** 115 (2001).
4. H. Walter, H. G. Kahle, K. Mulder, H. C. Schopper, and H. Schwarz, *Int. J. Magn.* **5,** 129 (1973).
5. E. Jiménez, J. Isasi, and R. Sáez-Puche, *J. Alloys Comp.* **312,** 53 (2000).
6. K. Tezuka and Y. Hinatsu, *J. Solid State Chem.* **160,** 362 (2001)

7. J. Rodríguez-Carvajal, Abstracts of the Satellite Meeting on Powder Diffraction of XVth Congress of the International. Union of Crystallography, Toulouse, France, 1990, p. 127.
8. L. N. Mulay and E. Boudreaux, "Theory of molecular paramagnetism," p. 494. Wiley, New York, 1976.
9. K. Yoshii and A. Nakamura, *J. Solid State Chem.* **155,** 447 (2000).
10. A. V. Mahajan, D. C. Johnston, D. R. Torgeson, and F. Borsa, *Physica C* **185–189,** 1195 (1991).
11. A. V. Mahajan, D. C. Johnston, D. R. Torgeson, and F. Borsa, *Phys. Rev. B* **46,** 10966 (1992).
12. N. Shirakawa and M. Ishikawa, *Jpn. J. Appl. Phys., Part 2* **30,** l7555 (1991).
13. J. B. Goodenough and H. C. Nguyen, *C. R. Acad Sci., Ser. Iib: Mec., Phys., Chim., Astron.* **319,** 1285 (1994).
14. Y. Ren, T. T. M. Palstra, D. I. Khomskii, A. A. Nugroho, A. A. Menovsky, and G. A. Sawatzky, *Phys. Rev. B* **62** (10), 6577 (2000).